agriculture

MDPI

Article

Safety Analysis of Fastening Device of Agricultural By-Product Collector in Various Ground Conditions

Jeong-Hun Kim [1,2], Markumningsih Sri [3], Seok-Joon Hwang [1,2], Moon-Kyeong Jang [1,2], Seung-Jun Kim [1,2], Yun-Jeong Yang [1,2] and Ju-Seok Nam [1,2,*]

[1] Department of Biosystems Engineering, College of Agricultural and Life Science, Kangwon National University, Chuncheon 24341, Republic of Korea; jhkim1995@kangwon.ac.kr (J.-H.K.); human51@naver.com (S.-J.H.); moon2842@kangwon.ac.kr (M.-K.J.); gracenav4@naver.com (S.-J.K.); yyj000501@naver.com (Y.-J.Y.)
[2] Interdisciplinary Program in Smart Agriculture, Kangwon National University, Chuncheon 24341, Republic of Korea
[3] Department of Agricultural and Biosystems Engineering, Faculty of Agricultural Technology, Universitas Gadjah Mada, Yogyakarta 55281, Indonesia; sri_markumningsih@ugm.ac.id
* Correspondence: njsg1218@kangwon.ac.kr; Tel.: +82-33-250-6497

Abstract: In this study, to evaluate the safety of the fastening device, which is a vulnerable part of the agricultural by-product collector, the stress in fastening devices was measured, and the operational and driving safety were analyzed by deriving the static safety factor and fatigue life. The position with the maximum stress in fastening devices was identified through structural analysis simulation, and a stress measurement system was constructed using strain gauges. Test conditions for stress measurement were classified into three operating conditions (collection operation, driving with the loading part lifted to the highest point, and driving with the loading part lifted to the lowest point) and three soil conditions (even pavement, sloped pavement, and farmland). A process for deriving the fatigue life based on the measured stress was constructed by applying the rain-flow counting method, Goodman equation, and Palmgren–Miner's rule via commercial software. From the stress measurement results, the collection operation exhibited the highest maximum stress, followed by driving with the loading part lifted to the highest point and driving with the loading part lifted to the lowest point. Under all conditions, the static safety factor of the fastening devices was found to be higher than 1.0 (1.16–1.33). The fatigue life of the fastening devices was also found to be longer than the service life of Korean agricultural machinery under all operating conditions. Therefore, the fastening devices are expected to operate safely under generated static and dynamic loads. The agricultural by-product collector can perform agricultural work and drive stably and is expected to contribute to reducing unnecessary labor force for Korean farms.

Keywords: agricultural by-product collector; rain-flow counting; static safety factor; fastening device; fatigue life

check for updates

Citation: Kim, J.-H.; Sri, M.; Hwang, S.-J.; Jang, M.-K.; Kim, S.-J.; Yang, Y.-J.; Nam, J.-S. Safety Analysis of Fastening Device of Agricultural By-Product Collector in Various Ground Conditions. *Agriculture* **2023**, *13*, 2064. https://doi.org/10.3390/agriculture13112064

Academic Editors: Chung-Liang Chang and Mustafa Ucgul

Received: 15 September 2023
Revised: 25 October 2023
Accepted: 25 October 2023
Published: 27 October 2023

1. Introduction

Recently, the necessity of developing alternative energy sources has been emphasized worldwide owing to the lack of fossil energy sources and reinforced environmental regulations on emissions [1]. Accordingly, attention has been paid to biomass, which uses agricultural by-products as fuel, as an alternative energy source in Korea [2], and studies have been conducted to produce and process biomass [3–6]. There are, however, few studies on agricultural machinery that can directly collect or process agricultural by-products, such as pruned branches. In this regard, Hwang et al. designed an agricultural by-product collector for pruned branches of fruit trees, which have the highest potential generation and potential energy among agricultural by-products produced in Korea [7]. Owing to the nature of the cultivation environment of fruit trees, large loads can arise because of irregular

road surface conditions and the vibration of the operating part during the operation and driving of the agricultural by-product collector [8]. Such loads may cause deformation and cracking in the collector, which may lead to damage to the vulnerable part. Therefore, safety analysis of agricultural by-product collectors is required to increase work safety and prevent damage and failure.

Fatigue failure refers to a fracture due to the accumulation of damage caused by the application of repeated stress to the material over an extended period of time [9–11]. Fatigue failure is mainly caused by cracking. Cracking, which is the first stage of fatigue failure, is caused by local plastic deformation that occurs inside the material. Cracks grow with repeated loads, and they eventually lead to the fracture of the material. In this instance, the number of repetitions or time of the load until the fracture of the material under cyclic loads is referred to as fatigue life. In fact, fatigue has mostly been reported as the cause of damage to machines and structures, and it causes human casualties and property damage [12]. To minimize such damage, it is necessary to predict and design the fatigue life of material as a reference [13]. This is important in the design of agricultural machinery. To accurately determine the fatigue life of agricultural machinery, it is necessary to derive the load and stress frequency that occur during actual agricultural work and driving. There are various techniques for deriving stress frequency. Among them, the representative technique is rain-flow counting. It is possible to derive the stress range, mean stress, and number of stress cycles using rain-flow counting and to predict fatigue life using the S-N curve—a characteristic of the material—and Palmgren–Miner's linear cumulative damage rule. Kulkarni et al. (2016) assessed fatigue life to analyze the effect of an increase in the mass of the switched reluctance motor (SRM), which is used in small vehicles, on suspension design [14]. Kim et al. (2018) measured the stress generated in the transplanter PTO axis according to the planting distance during transplanting and derived fatigue life by applying rain-flow counting [15]. Choi et al. (2020) conducted fatigue analysis on the tunnel boring machine (TBM) cutter head, which is the representative equipment of mechanized tunnel construction, to predict its fatigue life under cyclic load conditions [16]. Bohm and Kowalsk (2020) developed a fatigue test model for the case in which aluminum alloys are subjected to torsional loads with a certain amplitude through rain-flow counting and Palmgren–Miner's linear cumulative damage rule [17]. Han et al. (2022) derived the load acting on the differential gear under the application of braking loads, such as a sudden stop or start, using a tractor front-axle analysis model to evaluate safety [18]. As described, the fatigue life of components is derived to evaluate safety during the design of various machines, including agricultural machinery.

In this study, the stress in the fastening devices of the agricultural by-product collector was measured under various operating and soil conditions, and safety was evaluated by deriving the static safety factor and fatigue life. The stress measurement system was constructed by installation of a strain gauge in the location where the maximum stress generated on the fastening device. The static safety factor was derived based on the measured maximum stress. In addition, the dynamic safety and fatigue life were derived by applying the rain-flow counting, Goodman equation, S-N curve, and Palmgren–Miner's linear cumulative damage rule. As a result, it is judged that the application of the agricultural by-product collector to Korean farms will contribute to reducing farmers' labor force and increasing convenience.

2. Materials and Methods

2.1. Agricultural by-Product Collector [7]

In this study, the agricultural by-product collector consists of a collecting part, a transferring part, a loading part, and a driving part, as shown in Figure 1. The collecting part adopts the longitudinal axis rotation method to collect agricultural by-products in the middle using two rotating collection brushes. The transferring part transports the collected agricultural by-products from the ground to the loading part through a conveyor belt. The maximum capacity of the loading part is 100 kg, and the cargo box can be moved up and

down through the application of a lifting device [19]. The size of the cargo box was set to 900 × 1100 × 450 mm (W × L × H). Tracked wheels were applied to the agricultural by-product collector, so that it could travel on soft soil in a stable manner.

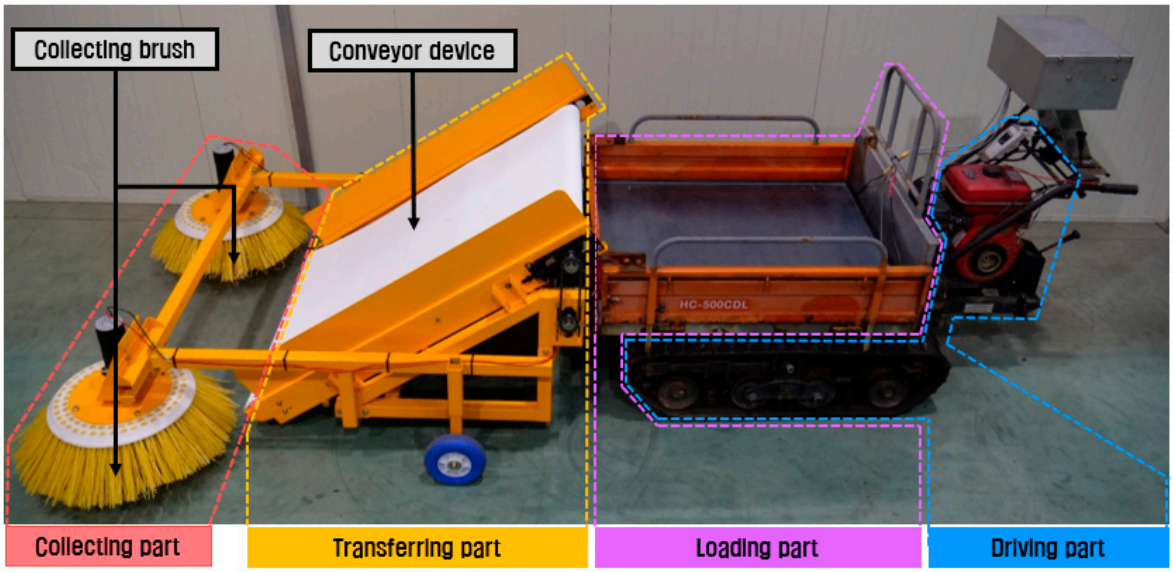

Figure 1. Shape of the agricultural by-product collector.

In the agricultural by-product collector, the transferring and the loading parts are combined by inserting two cantilever-type fastening devices connected to the transferring part frame into the hollow pipes located on the bottom frame of the loading part (Figure 2). The fastening devices were divided into the left (L) and right (R) devices, as viewed from the driving part toward the collecting part. The fastening devices must bear the self-weight of the collecting–transferring parts when the parts are raised from the ground, and they are subjected to variable loads during the collection operation due to the vibration caused by the stone, gravel, and obstacles on the ground. Considering that the fastening devices have structurally vulnerable cantilever geometry, their safety must be secured for the safe operation of the agricultural by-product collector.

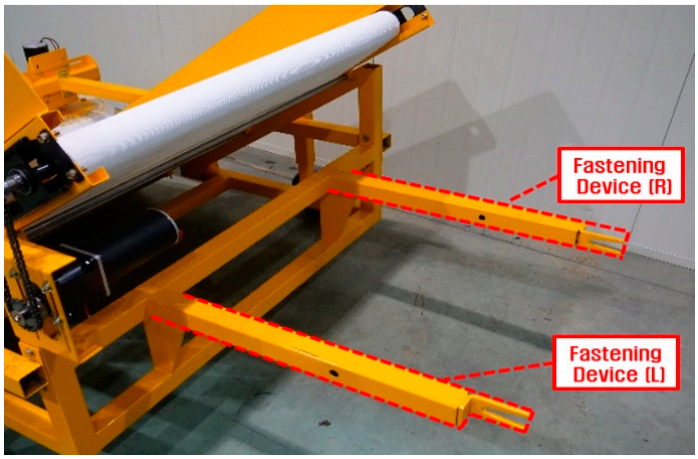

Figure 2. Shape of the fastening device.

2.2. Stress Measurement

2.2.1. Measurement System Configuration [20]

To evaluate the safety of the fastening devices, it is necessary to identify the position with the maximum stress and measure the stress at that position during the operation

of the agricultural by-product collector. Kim et al. (2022) conducted structural analysis through commercial dynamics simulation and derived the position with the maximum stress in the fastening device [19]. The position was the upper part of the fastening devices, 175 mm away from the transferring part frame. Therefore, in this study, strain gauges were installed in the position to measure the strain during the operation of the agricultural by-product collector (Figure 3). The measurement system was composed of strain gauges for measuring the axial vertical stress, a data acquisition system (DAQ), and a laptop for real-time display and storage of the measurement results (Figure 4). Also, the stress value measured through the data acquisition system shows an accuracy of 0.05–0.15% from the actual value.

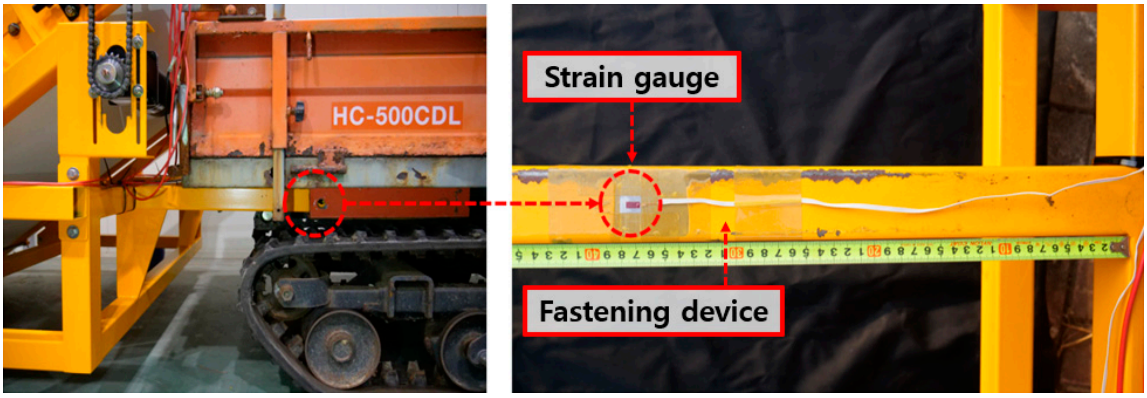

Figure 3. Attachment location of strain gauge.

Figure 4. Configuration of measurement system.

2.2.2. Test Conditions

The actual operating conditions of the agricultural by-product collector can be divided into collecting pruned branches of fruit trees and driving to the farmland. Therefore, the following three conditions were set as the operating conditions to measure the stress of the fastening devices: collection operation, driving with the loading part lifted to the highest point, and driving with the loading part lifted to the lowest point (Figure 5).

(**a**) (**b**) (**c**)

Figure 5. Driving conditions of agricultural by-product collector. (**a**) Collection operation. (**b**) Driving with the loading part lift-ed to the highest point. (**c**) Driving with the loading part lifted to the lowest point.

Considering the operating environment of the agricultural by-product collector, the following three soil conditions were selected: even pavement, sloped pavement, and farmland (Figure 6). The average ground slope of orchards in Korea ranges from 0 to 5°; however, a small number of orchards have a slope of approximately 16° to increase the drainage capacity of the ground [21]. Therefore, the slope of the sloped pavement was set to 16°, which is the harshest condition. The stress according to the three types of operation was measured under each soil condition, and the operating distance per test was set to 30 m. Under each condition, the average value of three repeated tests was used as the representative value. The driving speed of the agricultural by-product collector was fixed at 1.0 m/s by referring to a previous study [7].

(**a**)

(**b**) (**c**)

Figure 6. Soil conditions for stress measurement. (**a**) Even pavement. (**b**) Sloped pavement. (**c**) Farmland.

The soil from farmland was analyzed by soil sampling and classified as sand composed of clay (2.18%), silt (4.41%), and sand (93.41%). The average water content was found to

be 14.86% after measuring at six random locations on the farmland through the oven dry method.

2.3. Safety Analysis Method

2.3.1. Static Safety Factor

In mechanical design, uncertainties of material strength, machining precision, and workload must be considered, so that the designed product can have higher safety than the required performance or capability. In this instance, the safety of a machine under static loads is evaluated through the static safety factor. An increase in the safety factor involves an increase in cost and weight, while a decrease in the safety factor leads to higher risk. Therefore, it is necessary to set a proper static safety factor in the design of machine products, considering both the cost added by increasing the safety factor and the risk of damage. The stress-based static safety factor is defined as the ratio of the allowable strength of the material to the maximum stress acting on it. The stress acting on the material can be divided into shear stress, vertical stress, and equivalent stress. The yield strength of the material is generally applied as the allowable strength. Therefore, the static safety factor can be calculated as the ratio of the shear yield strength to the maximum shear stress for shear stress and as the ratio of the tensile yield strength to the maximum vertical stress/maximum equivalent stress for vertical and equivalent stress, respectively. In general, when the static safety factor exceeds 1.0, it can be said to be safe under static loads. If the maximum stress of a specific area is higher than the allowable strength of the material, the static safety factor becomes less than 1.0, and static damage may occur in the area, thereby causing failure or malfunction [22]. Since the fastening devices are mainly subjected to the uniaxial vertical stress caused by bending as a cantilever type, the static safety factor was derived using the tensile yield strength and Equation (1).

$$\text{S.F.} = \frac{S_y}{\sigma_{max}} \tag{1}$$

where

S.F. = Static safety factor;
S_y = Tensile yield strength of the material;
σ_{max} = Measured maximum normal stress during the operation.

2.3.2. Fatigue Life

Even a very lower load compared to the load that causes static damage may lead to the fracture of the material if applied repeatedly, due to the accumulation of damage. Fatigue life is a criterion for determining safety under repeated loads, and it means the number or time of load cycles until the fracture of the material due to the accumulation of damage. Fatigue life must be longer than the required service life for the stable operation of the system. Fatigue life is derived by applying rain-flow counting, the Goodman equation, and Palmgren–Miner's linear cumulative damage rule to the measured stress data in the time domain. The strain measured through the uniaxial strain gauge can be converted into vertical stress using Equation (2).

$$\sigma = E \times \varepsilon \tag{2}$$

where

σ = Measured normal stress;
E = Modulus of elasticity;
ε = Measured normal strain.

To derive fatigue life, it is necessary to convert the measured stress data in the time domain into the frequency domain and count the number of stresses of a certain amplitude. This is referred to as cycle counting. Cycle counting methods include level crossing counting, peak counting, and rain-flow counting. Among them, rain-flow counting has

been most widely used [23]. It is possible to obtain information on the stress amplitude, mean stress, and number of cycles by applying rain-flow counting to the stress data in the time domain. A life cycle must be derived by applying stress data that correspond to each level to the S-N curve of the material. To this end, the stress composed of the amplitude and average must be converted into the equivalent completely reversed stress with an average of zero. The equivalent completely reversed stress can be obtained through the Goodman equation, as shown in Equation (3).

$$\sigma_{eq} = \frac{S_u \times \sigma_a}{S_u - \sigma_m} \tag{3}$$

where

σ_{eq} = Equivalent completely reversed stress;
S_u = Ultimate tensile strength of the material;
σ_a = Measured stress amplitude;
Σ_m = Measured mean stress.

When the equivalent completely reversed stress is substituted into the S-N curve of the material, it is possible to obtain the life cycle corresponding to the completely reversed stress. The total damage sum can be calculated using Equation (4) by applying the number of actually applied cycles of the stress and life cycle to Palmgren–Miner's linear cumulative damage rule. The linear cumulative damage rule derives the total damage sum by adding the partial damage caused by all applied loads under the assumption that fatigue damage is linearly accumulated, and it assumes that the fatigue damage of the material occurs when the total damage sum becomes 1.0 [24]. The fatigue life based on the total damage sum (obtained via Equation (4)) can be calculated using Equation (5).

$$D_t = \sum_{i=1}^{k} \frac{n_i}{N_i} \tag{4}$$

where

D_t = Total damage sum;
n_i = Number of actually applied cycles for ith stress;
N_i = Life cycles for ith stress.

$$L_f = \frac{1}{D_t} \times t \tag{5}$$

where

L_f = Fatigue life;
D_t = Total damage sum;
t = Working time, which generates damage sum.

2.3.3. Process of Deriving Fatigue Life

Fatigue life was derived from the measured stress data in the time domain using nCode (nCode, Version 19.0.0, HBM Prencia, Southfield, MI, USA), a commercial software program. The process was constructed by applying the fatigue life calculation method described in Equations (3)–(5), so that the load spectrum and fatigue life can be derived by applying rain-flow counting, the Goodman equation, and Palmgren–Miner's linear cumulative damage rule when the stress data in the time domain are entered (Figure 7). The S-N curve of the fastening device material was selected based on the properties of the material and the library of the nCode software (Prenscia, nCode Book of Fatigue theory). The material was Steel UML UTS300. The properties and S-N curve of the material are presented in Table 1 and Figure 8.

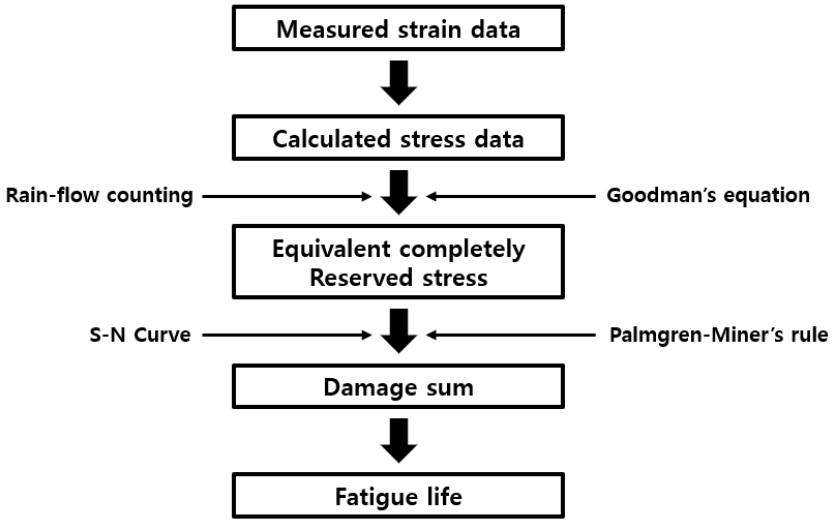

Figure 7. Theoretical analysis of fatigue life.

Table 1. Material properties of fastening device.

Item	Material Properties
Material	Steel UML UTS300
Yield strength (MPa)	231
Ultimate strength (MPa)	300
Elastic modulus (MPa)	2.07×10^5

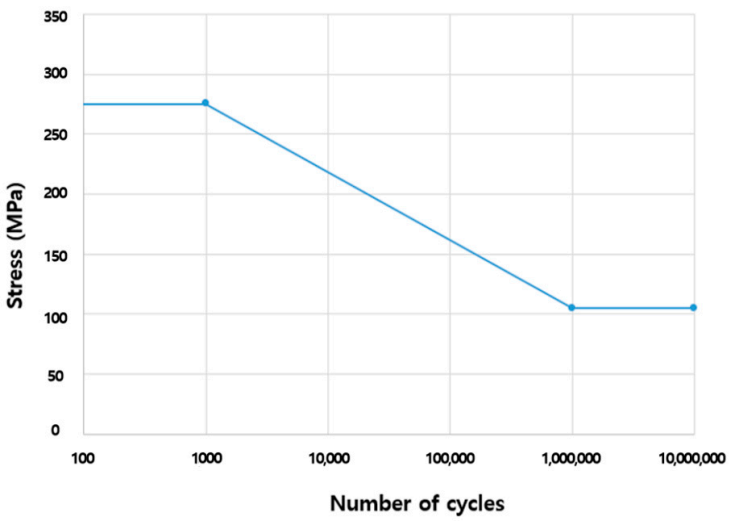

Figure 8. S-N curve for Steel UML UTS300.

3. Results and Discussion

3.1. Stress Measurement Results

The highest maximum stress in the fastening devices was measured during the collection operation on the farmland. The measured stress graphs in the time domain are shown in Figure 9. On farmland, the maximum stress exerted on each fastening device was 192.95–199.37 MPa (left) and 196.29–185.13 MPa (right). In case of the sloped pavement condition, the generated maximum stress was 187.60–180.79 MPa (left) and 181.96–175.98 MPa (right). The maximum stresses of 184.64–176.18 MPa (left) and 179.51–173.48 MPa (right) were measured in the even pavement condition.

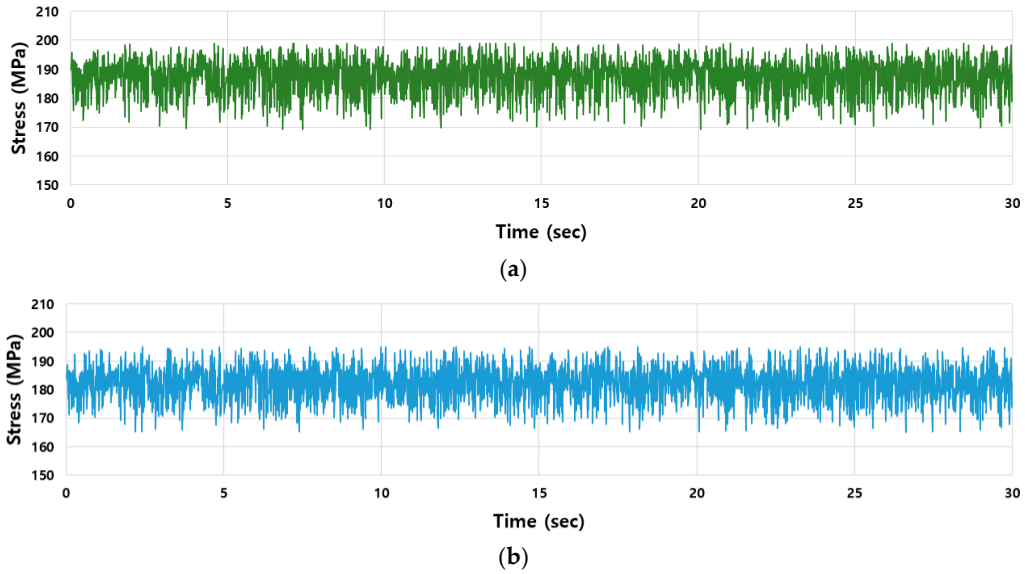

Figure 9. Time-series stress date of each fastening device during the collection operation on the farmland. (**a**) Fastening device (L). (**b**) Fastening device (R).

Regarding soil conditions, farmland exhibited the highest maximum stress, followed by sloped pavement and even pavement, in that order. It appears that high workloads were induced on the farmland because high vibration and impacts were generated in the fastening devices by the irregular road surface and obstacles. In addition, there was a relatively higher stress on the sloped pavement than on the even pavement. This appears to be because the load in the direction of the slope was additionally exerted on the fastening devices by the slope. Regarding the operating conditions, the collection operation exhibited the highest maximum stress, followed by the driving with the loading part lifted to the highest point and driving with the loading part lifted to the lowest point, in that order, under all soil conditions (Figure 10). It was found that the maximum stress during the collection operation was higher than that during driving with the loading part lifted to the highest point because the vibration caused by the collection operation had a larger impact than the moment load by the weight of the collecting and transferring parts.

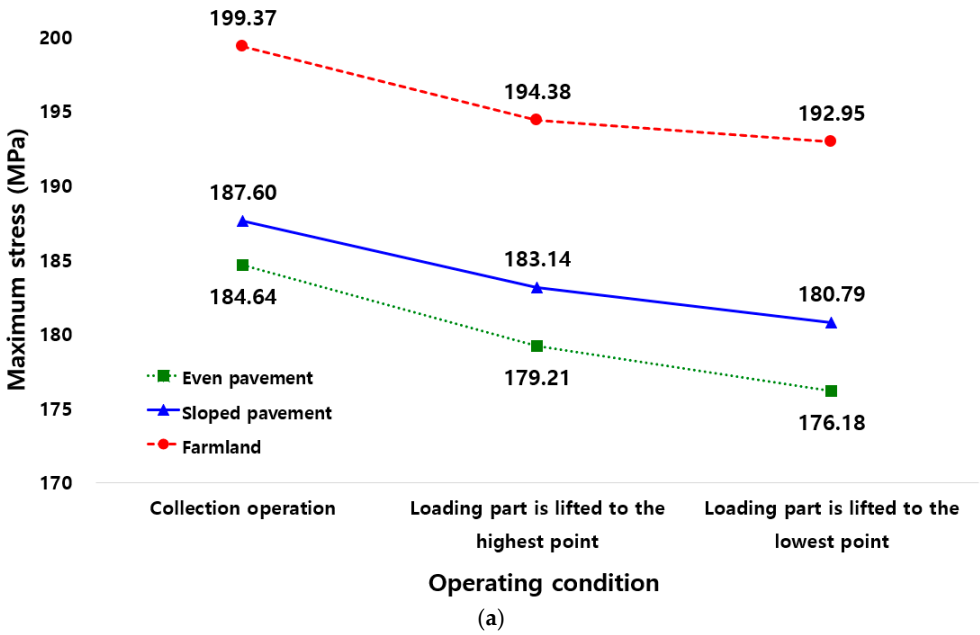

Figure 10. *Cont.*

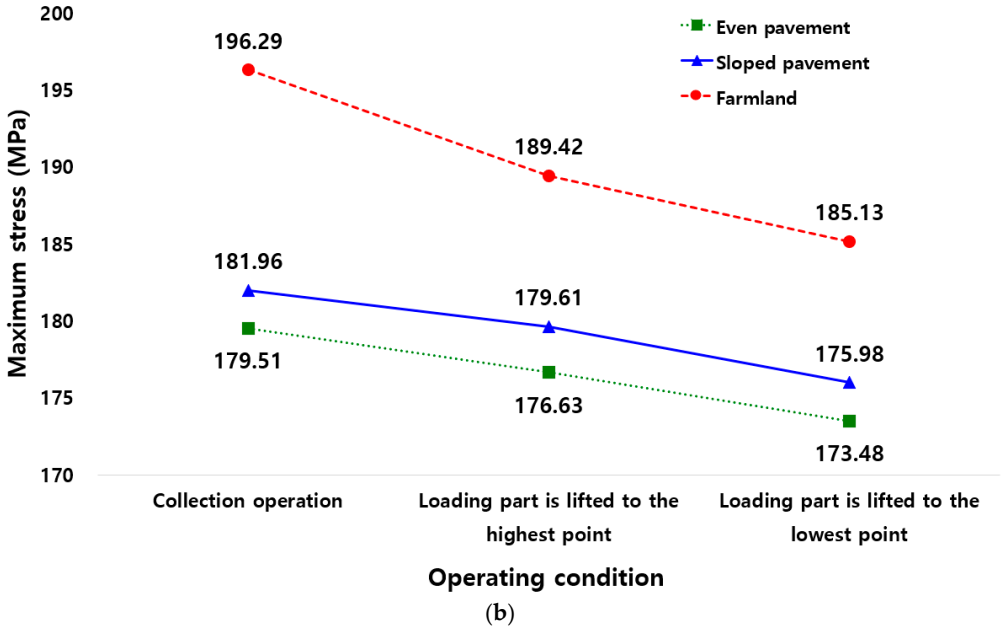

(**b**)

Figure 10. Measured maximum stress under each condition. (**a**) Fastening device (L). (**b**) Fastening device (R).

3.2. Results of Deriving Fastening Device Safety

3.2.1. Static Safety Factor

Based on the maximum stress derived under the test condition and the yield strength of the fastening device material, the static safety was derived. Table 2 summarizes the results of the static safety factor obtained via Equation (1). The static safety was found to be 1.16–1.29 for the collection operation, 1.19–1.31 for the driving with the loading part lifted to the highest point, and 1.21–1.33 for the driving with the loading part lifted to the lowest point. The operating condition with the lowest static safety factor was the collection operation on the farmland. In this case, the static safety factors were 1.16 and 1.18 for the left and right fastening devices, respectively. The static safety factor exceeded 1.0 under all test conditions, indicating that the fastening devices will operate safely, without damage under static loads.

Table 2. Static safety factor of the fastening device.

Driving Condition	Soil Condition	Fastening Device	
		L	R
Collection operation	Even pavement	1.25	1.29
	Sloped pavement	1.23	1.27
	Farmland	1.16	1.18
Loading part lifted to the highest point	Even pavement	1.29	1.31
	Sloped pavement	1.26	1.28
	Farmland	1.19	1.22
Loading part lifted to the lowest point	Even pavement	1.29	1.33
	Sloped pavement	1.29	1.33
	Farmland	1.21	1.25

3.2.2. Fatigue Life

The stress amplitude, mean stress, and number of cycles were derived by applying rain-flow counting to the measured time-series stress data under each test condition. The rain-flow counting results for the farmland-collection operation, which causes the highest stress, are shown in Figure 11. Under all operating and soil conditions, the mean stress

and stress amplitude for the fastening devices were found to be 155–200 MPa and 0–35 MPa, respectively. Stress conditions resulting in the maximum damage to the fastening devices are presented in Table 3. Under all test conditions, there was just one cycle that caused maximum damage, which was more than 70% of the total damage. This indicates that certain maximum-load conditions that occur during the operation and driving have decisive effects on damage and fatigue life.

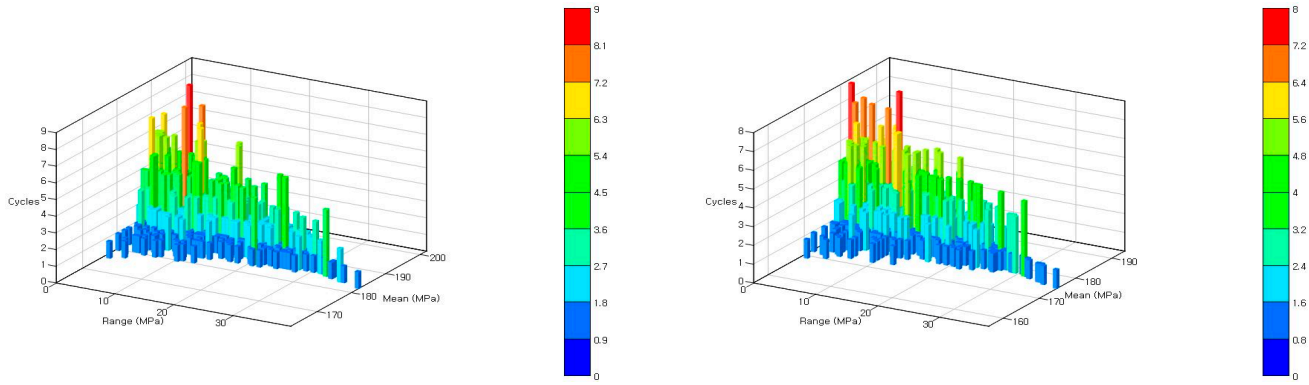

(**a**) (**b**)

Figure 11. Rain-flow counting result during the collection operation on the farmland. (**a**) Fastening device (L). (**b**) Fastening device (R).

Table 3. Maximum-damage condition for each fastening device.

Driving Condition	Soil Condition	Fastening Device	Mean Stress (MPa)	Stress Amplitude (MPa)	Equivalent Stress (MPa)	Damage	Number of Cycle
Collection operation	Even pavement	L	171.95	14.55	34.08	9.39×10^{-8}	1
		R	166.54	15.05	33.84	6.64×10^{-8}	
	Sloped pavement	L	168.34	18.95	43.18	3.17×10^{-7}	
		R	167.29	16.50	37.29	1.24×10^{-7}	
	Farmland	L	182.05	19.73	50.17	1.93×10^{-6}	
		R	174.78	18.76	44.94	5.91×10^{-7}	
Loading part lifted to the highest point	Even pavement	L	167.26	13.14	29.70	3.14×10^{-8}	1
		R	161.76	11.41	24.76	7.99×10^{-9}	
	Sloped pavement	L	173.01	12.02	28.40	3.35×10^{-8}	
		R	169.96	10.69	24.65	1.19×10^{-8}	
	Farmland	L	196.34	20.67	50.13	1.27×10^{-6}	
		R	171.96	18.39	43.09	3.85×10^{-7}	
Loading part lifted to the lowest point	Even pavement	L	161.31	11.69	25.29	8.88×10^{-9}	1
		R	159.71	10.85	23.19	4.90×10^{-9}	
	Sloped pavement	L	164.57	12.49	27.67	1.79×10^{-8}	
		R	160.97	11.72	25.28	8.72×10^{-9}	
	Farmland	L	171.35	20.48	47.75	6.89×10^{-7}	
		R	170.91	15.96	37.08	1.47×10^{-7}	

The load spectrum during the farmland-collection operation, which causes the highest stress, is shown in Figure 12. During the operation on the farmland, the number of cycles due to stresses below 10 MPa was less than 50%. It, however, exceeded 70% for operation on both the sloped and even pavements. In other words, the number of cycles due to stresses below 10 MPa increased with decreasing maximum stress, confirming that the farmland has the highest high-load occurrence rate, followed by sloped pavement and even pavement, in that order.

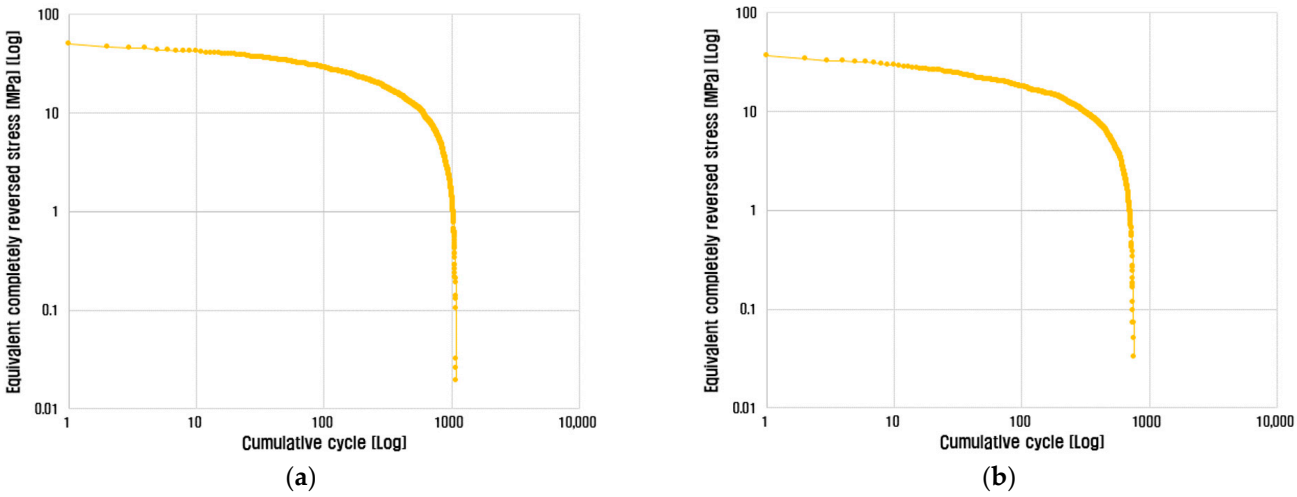

Figure 12. Load spectrum during the collection operation on the farmland. (**a**) Fastening device (L). (**b**) Fastening device (R).

Table 4 summarizes the total damage and fatigue life under each operation condition. Fatigue life was found to be shortest during the farmland-collection operation. The maximum stress tended to increase with decreasing fatigue life. In a literature review, the average annual pruning time of orchards in Korea was found to be 38.5 h [25]. Under the assumption that the agricultural by-product collector is continuously used during that time, the fatigue life of the fastening devices was found to be 621–2167 y for the collection operation, 1060–5041 y for driving with the loading part lifted to the highest point, and 2285–7205 y for driving with the loading part lifted to the lowest point. Considering that the average service life of agricultural machinery is 9 y [26], fastening devices of the agricultural by-product collector are expected to operate safely during their required service life, without damage under variable loads.

Table 4. Total damage and fatigue life of the fastening device.

Driving Condition	Soil Condition	Total Damage		Fatigue Life (hours)		Fatigue Life Considering 38.5 h of Annual Working Time (y)	
		Fastening Device (L)	Fastening Device (R)	Fastening Device (L)	Fastening Device (R)	Fastening Device (L)	Fastening Device (R)
Collection operation	Even pavement	8.094×10^{-7}	6.102×10^{-7}	1.277×10^{6}	1.932×10^{6}	33,168	50,181
	Sloped pavement	1.974×10^{-6}	1.251×10^{-6}	5.114×10^{5}	1.100×10^{6}	13,283	28,571
	Farmland	4.328×10^{-5}	1.212×10^{-5}	2.391×10^{4}	8.346×10^{4}	621	2167
Loading part lifted to the highest point	Even pavement	3.160×10^{-7}	1.358×10^{-7}	4.901×10^{6}	1.164×10^{7}	127,298	302,337
	Sloped pavement	2.072×10^{-7}	8.651×10^{-8}	3.209×10^{6}	7.907×10^{6}	83,350	205,376
	Farmland	2.645×10^{-5}	6.043×10^{-6}	4.084×10^{4}	1.941×10^{5}	1060	5041
Loading part lifted to the lowest point	Even pavement	3.464×10^{-7}	1.163×10^{-7}	1.175×10^{7}	1.986×10^{7}	305,194	511,168
	Sloped pavement	1.328×10^{-8}	6.503×10^{-9}	3.416×10^{6}	8.936×10^{6}	88,727	232,103
	Farmland	4.123×10^{-6}	1.382×10^{-6}	8.799×10^{4}	2.774×10^{5}	2285	7205

4. Conclusions

To analyze the safety of the agricultural by-product collector, the stress in the fastening devices—the vulnerable part of the collector—was measured, and the static safety factor, as well as fatigue life, was derived in this study. A stress measurement system based on strain gauges was constructed to measure the stress at the position with the maximum stress.

Three operating conditions (collection operation, driving with the loading part lifted to the highest point, and driving with the loading part lifted to the lowest point) and three soil conditions (even pavement, sloped pavement, and farmland) were selected as test conditions for stress measurement. Regarding soil conditions, farmland showed the highest maximum stress, followed by sloped pavement and even pavement. For the farmland, it appears that high stress was due to the vibration and impacts caused by the irregular road surface and obstacles. There was relatively higher stress on the sloped pavement compared with that on the even pavement, owing to the applied load in the direction of the slope by the slope. Regarding operating conditions, the collection operation exhibited the highest maximum stress, followed by driving with the loading part lifted to the highest point and driving with the loading part lifted to the lowest point. This indicates that the vibration caused by the collection operation has a significant impact on the stress of the fastening devices. In addition, when compared with the results derived from previous studies, the soil conditions were in the order of farmland, hard flat ground, sloped pavement, and even pavement. Based on the yield strength of the fastening device material and the maximum stress measured under each test condition, the static safety factor of the fastening devices was derived. The safety factor by operating condition was found to be 1.16–1.29 for the collection operation, 1.19–1.31 for driving with the loading part lifted to the highest point, and 1.21–1.33 for driving with the loading part lifted to the lowest point. It was judged that agricultural machinery is safe under static loads if the static safety factor of its vulnerable parts is higher than 1.0 during design by referring to a previous study. The static safety factor of the fastening devices exceeded 1.0 under all test conditions, indicating that the fastening devices will operate safely, without damage under static loads. The fatigue life of the fastening devices was found to be shortest during the collection operation on the farmland. Considering that the average annual pruning time of orchards in Korea is 38.5 y, the minimum fatigue life of the fastening devices is 621 y. Considering that the fatigue life of the fastening devices exceeds the average service life of agricultural machinery under all test conditions, the fastening devices are expected to operate safely during the required service life. The fatigue life of the fastening devices was much longer than their service life; however, the static safety factor was found to be less than 1.5, indicating that the fastening devices need to be designed with a focus on the static damage caused by the maximum load rather than the fatigue failure caused by variable loads. As future work, it is necessary to measure the stress generated in the fastening device and evaluate its safety when collecting agricultural by-products using the agricultural by-product collector in various agricultural fields.

Author Contributions: Theoretical and simulation analysis, J.-H.K., M.S., S.-J.H., M.-K.J., S.-J.K. and Y.-J.Y.; writing—original draft preparation, J.-H.K.; writing—review and editing, J.-S.N. All authors have read and agreed to the published version of the manuscript.

Funding: This work was supported by the Korea Institute of Planning and Evaluation for Technology in Food, Agriculture and Forestry (IPET) through the Machinery Mechanization Technology Development Program for Field Farming Program, funded by the Ministry of Agriculture, Food and Rural Affairs (MAFRA)(RS-2023-00235957).

Institutional Review Board Statement: Not applicable.

Data Availability Statement: Not applicable.

Conflicts of Interest: The authors declare no conflict of interest.

References

1. Jung, J.W.; Son, S.H.; Jang, Y.H.; Ryou, K.H.; Jeong, J.H.; Lee, S.Y.; Lee, S.M. *Structural Changes in the Global Energy Market and Diversification Policy in Korea's Energy Cooperation with the Middle East*; Korea Institute for International Economic Policy: Sejong, Republic of Korea, 2020.
2. Park, W.K.; Park, N.B.; Shin, J.D.; Hong, S.G.; Kwon, S.I. Estimation of Biomass Resource Conversion Factor and Potential Production in Agricultural Sector. *Korean J. Environ. Agric.* **2011**, *30*, 252–260. [CrossRef]

3. Cha, J.Y.; Ali, M.; Hong, Y.S.; Yu, B.K.; Lee, S.H.; Seonwoo, H.; Kim, H.J. Development of a Pelletizing System of Fermented TMR for Pig Feeding. *J. Biosyst. Eng.* **2018**, *43*, 119–127. [CrossRef]
4. Patel, D.K.; Kim, M.H.; Lim, K.T. Synthesis and Characterization of Eggshell-Derived Hydroxyapatite Bioceramics. *J. Biosyst. Eng.* **2019**, *44*, 128–133. [CrossRef]
5. Alahakoon, A.; Karunarathna, A.; Dharmakeerthi, R.; Silva, F. Design and Development of a Double-chamber Down Draft(DcDD) Pyrolyzer for Biochar Production from Rice Husk. *J. Biosyst. Eng.* **2022**, *47*, 458–467. [CrossRef]
6. Park, S.Y.; Kim, S.J.; Oh, K.C.; Jeon, Y.K.; Kim, Y.M.; Cho, A.Y.; Lee, D.H.; Jang, C.S.; Kim, D.H. Biochar from Agro-byproducts for Use as a Soil Amendment and Solid Biofuel. *J. Biosyst. Eng.* **2023**, *48*, 93–103. [CrossRef]
7. Hwang, S.J.; Kim, J.H.; Nam, J.S. Factorial Experiment for the Collecting Device of and Agricultural By-product Collector. *J. Biosyst. Eng.* **2020**, *45*, 422–431. [CrossRef]
8. Han, G.H.; Kim, D.K.; Ahn, D.V.; Park, Y.J. Comparative Analysis of Tractor Ride Vibration According to Suspension System Configuration. *J. Biosyst. Eng.* **2023**, *48*, 69–78. [CrossRef]
9. Vincent, M.K.; Varghese, V.; Sukumaran, S. Fabrication and Analysis of Fatigue Testing Machine. *Int. J. Eng. Sci.* **2016**, *5*, 15–19.
10. Jeong, S.U. Bending Fatigue Characteristics and Stress Analysis of STS304 Steel. *J. Inst. Mar. Ind.* **2007**, *20*, 79–84.
11. Kang, M.S.; Koo, J.M.; Seok, C.S.; Park, J.S. Fatigue Characteristic of High Impact Polystyrene(HR-1360). *Korean Soc. Mech. Eng. A* **2010**, *34*, 763–769. [CrossRef]
12. Yeom, H.H.; Jung, Y.C.; Kim, C.Y.; Kang, K.Y.; Lee, M.G.; Hong, M.S.; Jeon, Y.H. Ultrasonic Fatigue Test for a High Strength Steel Plate. *J. Korean Soc. Manuf. Technol. Eng.* **2015**, *24*, 589–593. [CrossRef]
13. Murakami, M.; Takai, T.; Wada, K.; Matsunaga, H. Essential structure of S-N curve: Prediction of fatigue life and fatigue limit of defective materials and nature scatter. *Int. J. Fatigue* **2021**, *146*, 106–138. [CrossRef]
14. Kulkarni, A.; Ranjha, S.A.; Kapoor, A. Fatigue analysis of a suspension far and in-wheel electric vehicle. *Eng. Fail. Anal.* **2016**, *68*, 150–158. [CrossRef]
15. Kim, W.S.; Kim, Y.S.; Kim, Y.J. Analysis of the Load of a Transplanter PTO Shaft Based on the Planting Distance. *J. Fac. Agric. Kyushu Univ.* **2018**, *63*, 97–102. [CrossRef]
16. Choi, S.W.; Kang, T.H.; Lee, C.H.; Chang, S.H. Fatigue Analysis for Structural Stability Review of TBM Cutterhead. *J. Korean Tunn. Undergr. Sp. Assoc.* **2020**, *22*, 529–541. [CrossRef]
17. Bohm, M.; Kowalski, M. Fatigue Life Estimation of Explosive Cladded Transition Joints with the Use of the Spectral Method for the Case of a Random sea state. *Mar. Struct.* **2020**, *71*, 102739. [CrossRef]
18. Han, H.W.; Oh, J.S.; Yoo, H.J.; Shim, S.B. Strength Evaluation of the Tractor Differential Case Under Braking Load. *J. Agric. Life Environ. Sci.* **2022**, *34*, 9–16. [CrossRef]
19. Kim, S.J.; Kim, J.H.; Nam, J.S. Performance Test of Agricultural By-product Collecting Monitoring System. *Precis. Agric. Sci. Technol.* **2022**, *4*, 71–80. [CrossRef]
20. Kim, J.H.; Sri, M.; Nam, J.S. Safety Evaluation on a Fastening Device of an Agricultural By-Product Collector for Hard Flat Ground Driving. *Agriculture* **2022**, *12*, 1071. [CrossRef]
21. Noh, J.S.; Cho, Y.J.; Kim, T.S.; Lee, D.H.; Lee, K.S. Driving Running Stability of Orchard Aerial Lift by Using Recurdyn that is Analysis Tool. *Proc. Korean Soc. Agric. Mach. Conf.* **2012**, *17*, 153–159.
22. Budynas, R.G.; Nisbett, J.K. *Shigley's Mechanical Engineering Design*, 9th ed.; Mcgraw-Hill: New York, NY, USA, 2011; pp. 10–15.
23. Park, J.J.; Seo, S.M.; Seo, M.W.; Choi, Y.S.; Kim, Y.J. Development of Material Properties Measurement and Fatigue Life Evaluation System. *Korean Soc. Mech. Eng. A* **1994**, *18*, 1465–1473.
24. Lee, W.S.; Lee, H.W. A Study on the Prediction of the Fatigue Life of a Lug through the Finite Element Analysis. *J. Korean Soc. Precis. Eng.* **1998**, *15*, 88–95.
25. Lee, Y.H.; Lee, J.H.; Lee, K.S.; Kim, K.R.; Lee, S.J. Ergonomic Risk Factors Related to Musculoskeletal Symptoms in the Vineyard Workers. *J. Korean Soc. Occup. Environ. Hyg.* **2008**, *18*, 122–132.
26. Lee, J.M.; Kim, Y.Y.; Hwang, S.J. *A Study of Useful Life for Agricultural Machinery*; National Institute of Agricultural Sciences: Wanju, Republic of Korea, 2017.